Published in Applied Physics Letters 90, issue 231111, 1-3, 2007
which should be used for any reference to this work

16.5 μm quantum cascade detector using miniband transport

Fabrizio R. Giorgetta,[a] Esther Baumann, Marcel Graf, Lassaad Ajili, Nicolas Hoyler, Marcella Giovannini, Jérôme Faist, and Daniel Hofstetter
University of Neuchâtel, 1 A.-L. Breguet, Neuchâtel CH 2000, Switzerland

Peter Krötz and Guido Sonnabend
I. Physikalisches Institut, Universität zu Köln, Zülpicher Straße 77, 50937 Köln, Germany

The authors report on an InP based photovoltaic quantum cascade detector operating at 16.5 μm and using miniband-based vertical transport. This concept allowed the construction of a longitudinal optical phonon extraction stair with two rungs without touching on a high device resistance. At 10 K, they observed a responsivity of 1.72 mA/W and a Johnson noise limited detectivity of 2.2×10^9 Jones. Altogether, this design resulted in detection at temperatures of up to 90 K with a lower bandwidth limit of 200 MHz imposed by the measurement setup.

Semiconductor infrared detectors based on an intersubband transition are widely explored not only because of the ability to tailor the device for a distinct and narrow detection energy range but also because of their ultrahigh speed capabilities.[1,2] Thanks to these properties, they are suitable for applications ranging from thermal imaging over midinfrared spectroscopy to industrial process monitoring. Recently, a 17 μm quantum cascade laser for astronomical applications, in particular, for infrared heterodyne spectroscopy on molecular hydrogen, has been demonstrated.[3] Since in this application the local oscillator will be a single-mode laser, the linewidth of the detector could be engineered to optimize its detectivity and to maximize the performance of the entire spectroscopic setup. Additionally, for such heterodyne experiments covering a reasonably large spectral range, this detector should ideally have large electrical bandwidth.

One of the standard detector types for such applications is the quantum well infrared photodetector (QWIP), which uses a bound to quasibound optical transition. A QWIP at 17 μm has been demonstrated by Sarusi *et al.* in 1994.[4] The photoconductive operation mode of such detectors normally implies that a bias voltage has to be applied; because of the finite device resistance, this results in a non-negligible dark current. Photovoltaic detectors, which operate without applied bias, do not suffer from dark current and the associated dark current noise. Roughly 10 years ago, a photovoltaic QWIP based on a graded barrier was proposed and built.[5–7] Yet another approach for photovoltaic intersubband light detection is provided by the quantum cascade detector (QCD).[8–14] Its operation is based on a bound to bound transition, whose excited state is coupled to an extraction cascade (phonon stair) transporting electrons vertically to the ground state of the following period.

Usually, a QCD consists of an active (doped) well, in which the optical transition between ground and first excited states defines the QCD's peak energy. The excited carriers are extracted by an extraction region consisting of a chirped superlattice, from where they are injected into the ground state of the next period's active well. Ideally, the extraction region is a phonon stair, whose step energies are close to the longitudinal optical phonon energy. This ensures a fast and efficient vertical carrier transport. For a detection energy around 75 meV (16.5 μm) and a longitudinal optical phonon energy of 34 meV (InGaAs), only two phonon steps are possible. This implicates an extraction cascade consisting of only one quantum well (QW)/barrier pair and results in strong coupling between adjacent active well ground states. As strong coupling leads to a large dark current, we have to minimize the overlap of the ground state wave functions of adjacent detector periods. Instead of a single QW/barrier pair, the center rung of the phonon stair consists in this case of a miniband formed by several quantum wells and barriers with similar thicknesses.

Consequently, we present here an InP-based QCD operating at 16.5 μm and making use of a miniband-type center rung. Figure 1 shows the self-consistently computed conduction band diagram of the structure. Incident photons with an energy of 70 meV are absorbed and excite electrons from the active well ground state A_1 to the miniband A_2/B_1 (transition energy=70 meV). The electron will then undergo a fast phonon-assisted transition to miniband C_1-F_1 formed by a very slightly chirped superlattice. Finally, the electron is in-

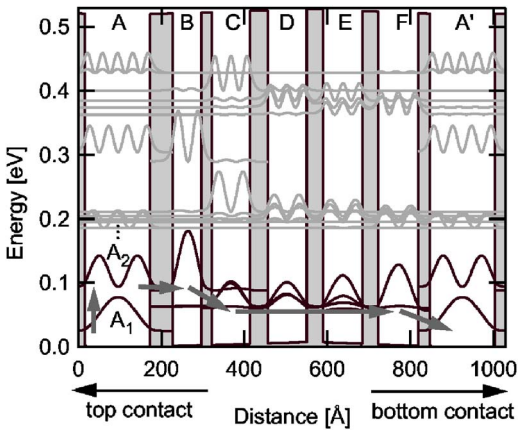

FIG. 1. Band structure of one period of the 16.5 μm QCD. $\mathbf{In_{53}Ga_{47}As}/In_{52}Al_{48}As$ layer thicknesses in angstrom from left to right: **157**/55/**69**/26/**90**/43/**94**/40/**95**/38/**96**/28. The arrows show the photocurrent path.

[a]Electronic mail: fabrizio.giorgetta@unine.ch

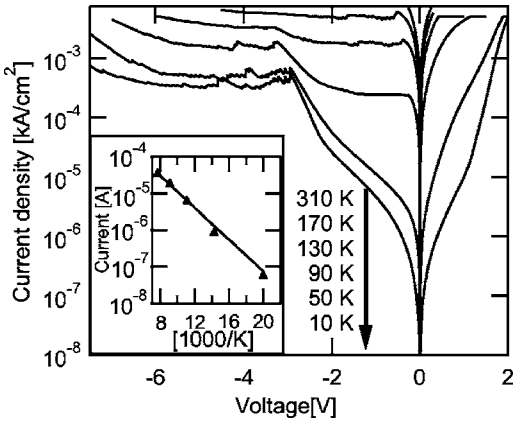

FIG. 2. *I-V* characteristics at different temperatures. Inset: Arrhenius plot. The extracted activation energy is 38 meV.

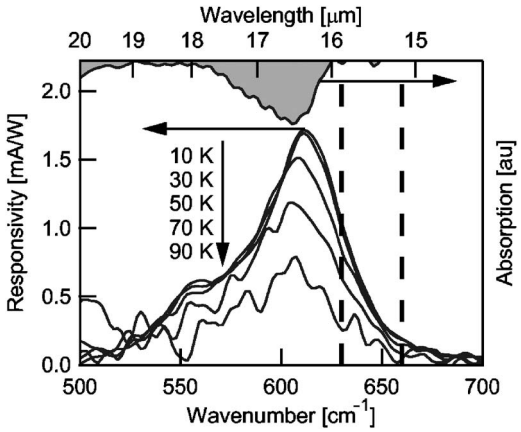

FIG. 3. Responsivity of sample with removed InP buffer at different temperatures. The signal peaks at 610 cm^{-1} is visible up to 90 K and has a maximal responsivity of 1.72 mA/W at 10 K. The two vertical dashed lines at 630 and 660 cm^{-1} represent the InP two-phonon absorption maxima. Also shown is the intersubband absorption hanging from the top axis.

jected into the next period's ground state A_1' by another phonon assisted tunneling transition. Since miniband transport as well as phonon assisted tunneling are processes involving time scales in the picoseconds range, high operation frequencies can be expected in such a device.

The sample was grown by molecular beam epitaxy on a semi-insulating InP substrate in order to minimize the free carrier absorption loss. Growth started with a 600 nm thick InGaAs:Si (3×10^{17} cm^{-3}) contact layer. The active region consists of a 157 Å wide active InGaAs well *n* doped to 1×10^{17} cm^{-3} followed by the extraction region, as shown in Fig. 1, and is repeated 30 times. X-ray measurements confirm that the effective superlattice period is within 2.1% and the barrier/well In content within 0.2% of the nominal values. The top contact was provided by another InGaAs:Si layer with identical doping as the lower contact and a thickness of 200 nm. An unannealed, highly *n*-doped contact was grown on top of the upper InGaAs layer. For device fabrication, square-shaped mesas with 200 μm side length were etched using standard photolithograpy and chemical wet etching in $HBr/H_2O_2/H_2O$-based (4:1:10) etch chemistry and Ohmic Ti/Ge/Au/Ti/Au (1.5/12/27/10/250 nm) top and bottom contact metals were deposited. The sample was then soldered on copper platelets and placed on the cold finger of a liquid He-flow cryostat. Finally, the cryostat was placed into the sample compartment of a Bruker IFS 66 Fourier transform infrared spectrometer. The photocurrent between the sample's top and bottom contacts was amplified with a SR 570 current amplifier and fed into the external detector port of the spectrometer. For current-voltage (*I-V*) characterization using a Keithley R2400 source meter, the sample was covered by the cryostats opaque radiation shield. Figure 2 shows the *I-V* characteristics at different temperatures. Positive voltages correspond to a positive potential at the top contact and therefore a positive conduction band slope in Fig. 1. For 10, 50, and 90 K, negative differential resistance (NDR) features set in at a voltage of −3 V at the top contact, whereas at 130 and 170 K, additional NDR features occur for voltages below −0.38 V. When computing the band structure with a superimposed electric field of $E_{\text{ext}}=-1.2$ V/μm corresponding to a potential difference of −3 V across the active region, the ground state A_1 comes into resonance with the second extraction cascade state D_1 of the same period. At higher voltages, each period sequentially breaks of from this resonance condition resulting in multiple NDR peaks. At higher temperatures, the current through the miniband increases significantly due to thermal excitation, resulting in additional low-voltage NDR features due to resonances in the extraction miniband. An Arrhenius plot of the current at 50 mV results in an activation energy of $E_{\text{act}}=38$ meV for the transport, which corresponds to the energy separating the ground state from the extraction miniband, a clear indication for leakage current across the miniband.

Figure 3 shows both absorption and responsivity spectra of the investigated material. In order to minimize the influence of InP two-phonon features in the absorption experiment, a relatively small (200 μm thick and 500 μm long) 45° multipass waveguide was polished. For normalization purposes, the active region was removed on part of the sample. The 10 K absorption spectrum hanging from the top *x* axis in Fig. 3 peaks at 605 cm^{-1} and is 34 cm^{-1} wide. Due to the sample's small size, stray light problems made it impossible to extract a meaningful value for the absorption efficiency. Although the optical path length in the sample is only 700 μm, the intersubband peak overlaps partly with the two-phonon absorption at 632 and 660 cm^{-1}, resulting in an asymmetric shape with a steeper drop at higher energy.

For responsivity measurements, the InP buffer was removed using HCl in order to avoid InP two-phonon absorption. The drawback of this process is the low amount of TM polarized light in the active region due to the small angle of 13° between incident light and growth axis, resulting in a low responsivity and thus detectivity values. At 10 K, the responsivity peaks at 610 cm^{-1} (16.4 μm/76 meV) exhibits a linewidth of 41 cm^{-1}, and thus has a relative linewidth of 7%. The responsivity R_0 in A/W was determined by

$$R_0=\frac{i_m}{P_m}\frac{4}{T},$$

with i_m the measured current density spectrum in A/m^2 *d* cm^{-1}, P_m the power density spectrum incident on the detector in W/m^2 *d* cm^{-1} as measured with a pyroelectric detector, and $T=0.85$ the transmission across the detector surface. The factor 4 accounts for the cryostats ZnSe window transmission and the unpolarized light. Based on these parameters, we obtained a value of $R_0=1.72$ mA/W at

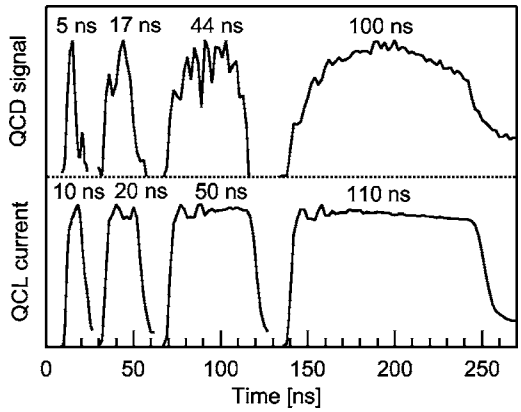

FIG. 4. Signal of the detector illuminated by a pulsed 17 μm quantum cascade laser. Bottom: normalized laser drive current. Top: Normalized detector signal.

610 cm^{-1} and 10 K. Similar as in a QWIP, the current responsivity is given by

$$R_0 = \frac{q}{h\nu}\eta\frac{p_e}{Np_c}.$$

With R_0=1.72 mA/W, p_c=1 the capture probability, q the elementary charge, $h\nu$=75 meV the peak photon energy, η =0.035 the calculated absorption efficiency for one double pass, and N=30 the number of periods, we obtain an escape probability of p_e=0.11. This value is rather low for a QCD and should increase with a more precise alignment of the A_2 and B_1 states. Although internal quantum efficiency, absorption efficiency, and gain are constant with temperature, the responsivity decreases by a factor of 2 between 10 and 90 K. Above 90 K, the signal disappears rapidly in the noise floor. As outlined earlier, the main reason for this effect is the thermally activated increase of the device conductivity via population of more strongly coupled quantum states, in particular, the miniband states.

Other transitions such as A_1 to A_4 or A_1 to the continuum at 2400 and at 4150 cm^{-1} (298 meV/4.15 μm and 514 meV/2.4 μm, respectively) are also visible, but they give small signal below 0.07 mA/W. At 10 K, the detectivity D^* amounts to 2.2×10^9 Jones and is Johnson noise limited as for earlier QCDs. Even at this low temperature, the detector does not reach its background limited regime of $D^*_{\mathrm{BLIP}}=2.2\times10^{10}$ Jones assuming a full-cone angle of 90°. The dominating Johnson noise also limits the high temperature operation severely, as the resistance drops by almost one order of magnitude within a small temperature range between 90 and 150 K.

To obtain a first estimation of the detector speed, its response to a pulsed 17 μm QCL was measured at 10 K. For this experiment, the QCD photocurrent was amplified with a Miteq AFS5-00102000-30-10P-4 amplifier in series with a Sonoma 317 amplifier. Figure 4 shows QCL drive current pulses of different lengths and the QCD's response to it, both measured with an oscilloscope. The shortest optical pulse width measured is 5 ns, resulting in a QCD bandwidth of at least 200 MHz. As the QCL drive current electronics did not allow for shorter pulses, this value can be regarded as a lower limit for the true bandwidth, which, based on the results from a similar device detecting at 5.35 μm,[14] is supposed to be in the gigahertz range. The smaller width of the measured QCD pulses compared to the drive current pulses can be explained by a retardation of lasing onset owing to the nonideal current pulse flank.

Compared to the first demonstration of a 17 μm QWIP dating from 1994,[4] we observe a detectivity of 2.2×10^9 Jones (Sarusi *et al.*: 1.7×10^{10} Jones). Due to the inherent lack of photoconductive gain, the responsivity of the QCD is roughly a factor of 17 smaller than the one of the QWIP. As far as the measurement speed is concerned, our device has clearly demonstrated rise and fall times better than 5 ns whereas no data are available for the QWIP. Based on the similar detection mechanism of the two device types, we do not expect that an optimized QCD at this wavelength will have a slower response than a QWIP. However, we anticipate that an improved design with a higher-lying miniband will lead to a considerably higher escape probability and resistance, and thus result in both an increased responsivity and detectivity of the device. Also, designing the structure for a longer detection wavelength around 17.1 μm will shift the intersubband transition away from the two-phonon absorption, allowing for a 45° waveguide to increase the responsivity by a factor of up to 13.

In conclusion, we have demonstrated that infrared detection based on InP-lattice matched QCDs is possible at long wavelengths up to 16.5 μm. Thanks to a vertical miniband transport in the extraction cascade, the device maintained a high resistance up to 100 K and therefore functioned at temperatures up to 90 K. A peak responsivity and Johnson noise limited detectivity of 1.72 mA/W and 2.2×10^9 Jones, respectively, were seen at 10 K. Similar with the earlier fabricated short wavelength QCDs, the full width at half maximum of the detection peak was small, namely, on the order of 41 cm^{-1}; this resulted in a relative linewidth of 7%. By using a 17 μm QCL operating at short current pulses, a setup limited maximum operation frequency of 200 MHz was determined.

The authors would like to thank the Professorship Program of the Swiss National Science Foundation for its generous financial support.

[1] H. C. Liu, J. M. Brown, K. Z. McIntosh, K. B. Nichols, and M. J. Manfra, Appl. Phys. Lett. **67**, 1594 (1995).
[2] P. D. Grant, R. Dudek, L. Wolfson, M. Buchanan, and H. C. Liu, Electron. Lett. **41**, 214 (2005).
[3] M. Rochat, D. Hofstetter, M. Beck, and J. Faist, Appl. Phys. Lett. **79**, 4271 (2001).
[4] G. Sarusi, S. D. Gunapala, J. S. Park, and B. F. Levine, J. Appl. Phys. **76**, 6001 (1994).
[5] B. F. Levine, S. D. Gunapala, and R. F. Kopf, Appl. Phys. Lett. **58**, 1551 (1991).
[6] C. Schönbein, H. Schneider, G. Bihlmann, K. Schwarz, and P. Koidl, Appl. Phys. Lett. **68**, 973 (1996).
[7] H. Schneider, C. Schönbein, G. Bihlmann, P. Van Son, and H. Sigg, Appl. Phys. Lett. **70**, 1602 (1997).
[8] L. Gendron, C. Koeniguer, X. Marcadet, and V. Berger, Infrared Phys. Technol. **47**, 175 (2005).
[9] L. Gendron, C. Koeniguer, V. Berger, and X. Marcadet, Appl. Phys. Lett. **86**, 121116 (2005).
[10] M. Graf, G. Scalari, D. Hofstetter, J. Faist, H. Beere, E. Linfield, D. Ritchie, and G. Davies, Appl. Phys. Lett. **84**, 475 (2004).
[11] D. Hofstetter, M. Beck, and J. Faist, Appl. Phys. Lett. **81**, 2683 (2002).
[12] L. Gendron, M. Carras, A. Huynh, V. Ortiz, C. Koeniguer, and V. Berger, Appl. Phys. Lett. **85**, 2824 (2004).
[13] M. Graf, N. Hoyler, M. Giovannini, J. Faist, and D. Hofstetter, Appl. Phys. Lett. **88**, 241118 (2006).
[14] D. Hofstetter, M. Graf, T. Aellen, J. Faist, L. Hvozdara, and S. Blaser, Appl. Phys. Lett. **89**, 061119 (2006).